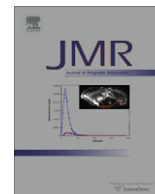




Contents lists available at SciVerse ScienceDirect

Journal of Magnetic Resonance

journal homepage: www.elsevier.com/locate/jmr

A spectrometer designed for 6.7 and 14.1 T DNP-enhanced solid-state MAS NMR using quasi-optical microwave transmission

Kevin J. Pike^{a,*}, Thomas F. Kemp^a, Hiroki Takahashi^a, Robert Day^a, Andrew P. Howes^a, Eugeny V. Kryukov^a, James F. MacDonald^a, Alana E.C. Collis^c, David R. Bolton^a, Richard J. Wylde^e, Marcella Orwick^d, Kosuke Kosuga^f, Andrew J. Clark^c, Toshitaka Idehara^f, Anthony Watts^d, Graham M. Smith^b, Mark E. Newton^a, Ray Dupree^{a,*}, Mark E. Smith^{a,1}

^a Department of Physics, University of Warwick, CV4 7AL, United Kingdom

^b School of Physics and Astronomy, University of St. Andrews, KY16 9SS, United Kingdom

^c Department of Chemistry, University of Warwick, CV4 7AL, United Kingdom

^d Biochemistry Department, University of Oxford, South Parks Road, Oxford OX1 3QU, United Kingdom

^e Thomas Keating Ltd., Billingshurst, W. Sussex RH14 9SH, United Kingdom

^f Research Center for Development of Far-Infrared Region, University of Fukui, 3-9-1 Bunkyo, Fukui 910-8507, Japan

ARTICLE INFO

Article history:

Received 26 July 2011

Revised 1 December 2011

Available online xxxxx

Keywords:

Dynamic Nuclear Polarisation

Signal enhancement

Magic Angle Spinning

Quasi-Optic Microwaves

ABSTRACT

A Dynamic Nuclear Polarisation (DNP) enhanced solid-state Magic Angle Spinning (MAS) NMR spectrometer operating at 6.7 T is described and demonstrated. The 187 GHz TE₁₃ fundamental mode of the FU CW VII gyrotron is used as the microwave source for this magnetic field strength and 284 MHz ¹H DNP-NMR. The spectrometer is designed for use with microwave frequencies up to 395 GHz (the TE₁₆ second-harmonic mode of the gyrotron) for DNP at 14.1 T (600 MHz ¹H NMR).

The pulsed microwave output from the gyrotron is converted to a quasi-optical Gaussian beam using a Vlasov antenna and transmitted to the NMR probe via an optical bench, with beam splitters for monitoring and adjusting the microwave power, a ferrite rotator to isolate the gyrotron from the reflected power and a Martin–Puplett interferometer for adjusting the polarisation. The Gaussian beam is reflected by curved mirrors inside the DNP-MAS-NMR probe to be incident at the sample along the MAS rotation axis. The beam is focussed to a ~1 mm waist at the top of the rotor and then gradually diverges to give much more efficient coupling throughout the sample than designs using direct waveguide irradiation. The probe can be used in triple channel HXY mode for 600 MHz ¹H and double channel HX mode for 284 MHz ¹H, with MAS sample temperatures ≥85 K. Initial data at 6.7 T and ~1 W pulsed microwave power are presented with ¹³C enhancements of 60 for a frozen urea solution (¹H–¹³C CP), 16 for bacteriorhodopsin in purple membrane (¹H–¹³C CP) and 22 for ¹⁵N in a frozen glycine solution (¹H–¹⁵N CP) being obtained. In comparison with designs which irradiate perpendicular to the rotation axis the approach used here provides a highly efficient use of the incident microwave beam and an NMR-optimised coil design.

© 2011 Elsevier Inc. All rights reserved.

1. Introduction

The sensitivity of Nuclear Magnetic Resonance (NMR) is limited by the thermal polarisation of the magnetic moments of nuclei even at high magnetic field strengths (~20 T). Dynamic Nuclear Polarisation (DNP) transfers polarisation from the much larger electronic magnetic moments to nuclei, which opens the possibility for NMR signals to be increased in strength by the ratio of the corresponding

gyromagnetic ratios, $|\gamma_S/\gamma_I| \sim 10^3$. This enhancement is defined by Eq. (1) where ε is the DNP enhancement, and I_{enh} and I_0 are the integrated intensities of the enhanced and thermal equilibrium spectra.

$$\varepsilon = \frac{I_{\text{enh}} - I_0}{I_0} \quad (1)$$

DNP was first predicted by Overhauser in 1953 [1] and confirmed experimentally at low magnetic field ($B_0 < 1$ T) shortly thereafter. The polarisation transfer mechanism used in this early work is now called the Overhauser Effect (OE), which occurs when nuclear spins and unpaired electronic spins are in relative motion. This process is therefore important for DNP in liquids, conductors and semiconductors. The electronic spins must be irradiated near

* Corresponding authors. Fax: +44 24 7652 3400.

E-mail addresses: Kevin.Pike@warwick.ac.uk (K.J. Pike), r.dupree@warwick.ac.uk (R. Dupree).

¹ Now at Lancaster University, Bailrigg, Lancaster LA1 4YW, United Kingdom.

their resonant frequency [2] and their polarisation must be at least partially saturated. Further investigation revealed other mechanisms including the Solid Effect (SE) [3,4] which still requires irradiation of the electronic spins, but does not need itinerant motion and is therefore applicable to other classes of solid. Development of DNP for use with the magnetic field strengths used for modern NMR spectroscopy ($B_0 \gg 1$ T) has needed to address two general problems: the decreasing effectiveness of the OE and SE with increasing field strength [5,6] and the availability of appropriate microwave sources, e.g. DNP at 10 T requires a microwave frequency of 280 GHz.

Further mechanisms for DNP in solids have been discovered that can be more effective at high fields [6], including the Cross Effect (CE) [7–9] and Thermal Mixing (TM) [2,10] that involve two and many electronic spins respectively. For optimal efficiency these mechanisms require different unpaired electron configurations, and biradicals containing two electronic spins have been designed specifically for CE DNP [11,12].

Several types of spectrometer systems have been developed for use with the microwave sources available with some designs using a lower field for the DNP enhancement and a higher field for the NMR detection. Dissolution DNP [13,14] involves irradiating a material with microwaves at $T \leq 4$ K in a lower field and then flushing it into a higher field with a warm liquid for a one-shot liquid-state NMR experiment. For shuttling DNP [15], samples are mechanically moved without change of state or temperature. Lower frequency microwave sources can be used for these techniques and large increases in nuclear polarisation are more easily achieved. Although electronic-spin polarisation at a given temperature is smaller in lower fields, dissolution DNP benefits from the large Boltzmann factor at low temperatures such that $\epsilon \sim 10^4$ can be achieved (with $\sim 10^2$ from DNP and $\sim 10^2$ from temperature) in a one-shot experiment. However, signal averaging (and therefore standard phase cycling) and standard 2D NMR spectroscopic techniques cannot be used.

More conventional NMR spectrometer configurations where the sample is irradiated with microwaves whilst in the NMR magnetic field can benefit from new high-frequency high-power microwave sources. Extended Interaction Klystrons (EIKs) have been used for DNP-NMR for field strengths up to 3.4 T [16,17] and gyrotrons for higher fields [6,18]. The transition probabilities causing SE DNP vary as B_0^{-2} so samples must be designed for use with CE and TM at these higher field strengths. DNP Magic Angle Spinning (MAS) NMR spectroscopy has been demonstrated at 5, 8.9 and 9.4 T using 140, 250 and 263 GHz gyrotrons (210, 380 and 400 MHz ^1H NMR, respectively) with $\epsilon \sim 100$ observed at $T < 100$ K using biradicals as the polarising agent [6,19,20].

In this paper we describe a DNP-enhanced solid-state NMR spectrometer designed for use at both 6.7 and 14.1 T (284 and 600 MHz ^1H NMR) that uses a gyrotron microwave source (187 GHz fundamental, 395 GHz second harmonic) and a quasi-optical system to transmit the microwaves to a MAS NMR probe capable of sample temperatures < 90 K. Results are presented for DNP-MAS-NMR at 6.7 T using the higher-power 187 GHz gyrotron mode and the effectiveness of the sample irradiation method is compared with that for other systems.

2. DNP-enhanced MAS NMR spectrometer

A schematic diagram of the spectrometer is shown in Fig. 1. The microwave source is the FU CW VII gyrotron whose operation has been described previously which can provide up to 150 W at 187 GHz TE₁₃ fundamental and 25 W at 395 GHz TE₁₆ second-harmonic in pulsed (quasi-CW) mode operation [21]. These microwave frequencies correspond to 284 and 600 MHz ^1H NMR

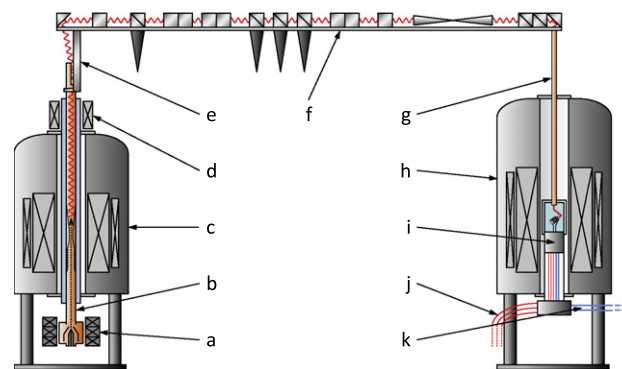


Fig. 1. Schematic representation of the high-field DNP-NMR spectrometer: (a) gun coils, (b) gyrotron tube, (c) 9.2 T gyrotron magnet with superconducting sweep coil, (d) electron collector solenoid, (e) Vlasov antenna, (f) quasi-optical microwave system, (g) corrugated waveguide, (h) 14.6 T NMR magnet and superconducting sweep coil, (i) cryo-MAS NMR probe, (j) RF cables, (k) cold N_2 gas for MAS bearing and drive.

frequencies, respectively. It uses a Varian superconducting 89 mm bore magnet with a maximum field strength of 9.2 T and a ± 0.2 T sweep coil. This sweep coil has a persistent-mode switch to allow choice of different modes whilst keeping the main coil in persistent mode to reduce helium consumption. Due to the need for high stability of the output power of the gyrotron the power supplies for the cathode (20 kV, 500 mA), the anode (20 kV, 20 mA), the heater and the gun coils were made in-house and have a stability of better than 1 in 10^4 . The cathode voltage is typically 12–15 kV and a high voltage switch allows the gyrotron to be operated in continuous wave (CW) or pulsed mode with a minimum delay between switching of 10 ms. Pulses typically have durations between 10 and 350 ms and can either be controlled by the NMR spectrometer console or a dedicated pulse generator.

The microwaves are transmitted as a quasi-optical Gaussian beam for most of the transmission length from the gyrotron to the NMR probe because the minimum distance between the two magnet centres due to their stray fields is almost 5 m. The transmission optics are shown in more detail in Figs. 2 and 3, and are calculated to have a total loss of 5 dB at 395 GHz. The quasi-optical system is designed to allow control of the microwave polarisation at the sample, as well as monitoring of the power level, purity, frequency, etc. Although the system is optimised for transmission of 395 GHz, only minor changes are necessary for 187 GHz operation. Quasi-optical transmission hardware has previously been used for DNP NMR for static samples with a low-power diode microwave source where low-loss transmission is critical [12].

The microwaves are launched through a sapphire window at the top of the gyrotron tube and converted into a beam by a Vlasov antenna [22], which consists of a launcher and two mirrors as shown in Fig. 3a. The launcher has a vertically-bisected cylindrical surface that radiates the approximately linearly polarised microwaves into free space at an angle of propagation which is dependent on the frequency and the mode supported in the gyrotron waveguide output. The microwaves are then reflected by a vertical cylindrical-elliptical mirror (M1 in Fig. 3a) and an orthogonal adjustable cylindrical-parabolic mirror (M2 in Fig. 3a). M1 is mounted close to the launcher and focuses the horizontal projection of the rapidly diverging beam, whilst M2 focuses the orthogonal projection of the beam shown in Fig. 3a. The combined effect of M1 and M2 is to create an approximately symmetrical Gaussian beam propagating horizontally with a ~ 4 mm waist (defined as the $1/e$ amplitude radius) for 395 GHz, (~ 8 mm for 187 GHz) at the first polarising grid (2 in Fig. 2).

After this initial conversion to a linearly polarised beam, there are a series of flat and ellipsoidal mirrors which ensure that the

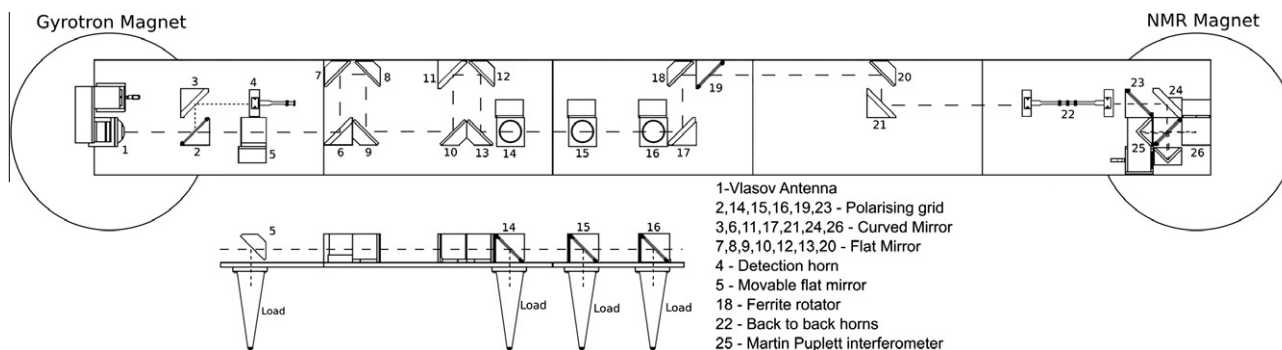


Fig. 2. Quasi-optical microwave transmission system. A low-loss transmission system from the gyrotron microwave source to the DNP enhanced NMR system.

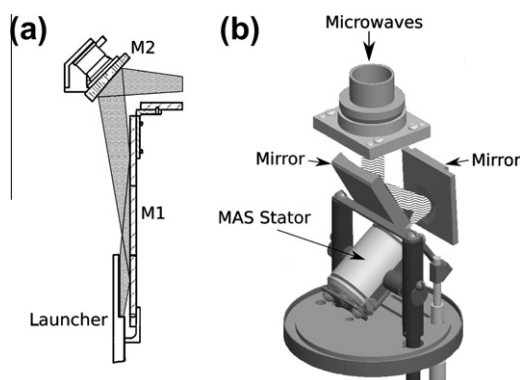


Fig. 3. (a) Vlasov antenna, (b) schematic showing path of microwaves into the rotor of the Magic Angle Spinning NMR probe.

propagating beam has the desired waist at the apertures of the horns (4 and 22 in Fig. 2) and corrugated waveguide ((g) in Fig. 1). As well as determining the polarisation of the beam the polarising grids allow control of the power level with excess power being dumped into the load cones (lower section of Fig. 2), which are cooled by water baths. For instance a single linear polarisation is transmitted by grid 14 to a rotatable polarising grid, 15, and then to grid 16. These form a variable attenuator with their relative orientations allowing control of the power delivered to the probe. The back-to-back horns, 22, act as a band-pass filter and re-launch the microwaves with a well defined polarisation into a set of optics that includes a Martin-Puplett Interferometer [23]. Adjustment of the position of a movable set of mirrors allows the interferometer to select linear or circular polarisation for transmission to the corrugated waveguide and the MAS NMR probe. The Faraday ferrite rotator, 18, in combination with the polariser grids 16 and 19 form a transmission mode isolator since the ferrite rotates the incoming linear polarisation by 45° which is then passed through polarising grid 19. Any power which is reflected back from the probe will have a known polarisation once it has passed grid 19 that will then be rotated by the ferrite rotator so that it has a polarisation which is 90° to the orientation of grid 16 and will therefore not be transmitted. Thus no power is reflected from the probe back to the gyrotron, protecting it from damage due to poor coupling to the corrugated waveguide, the MAS probe or the sample holder.

The quasi-optical transmission system uses sum-of-focal-length dimensions that allow most of its components to be inherently frequency-independent and therefore only minor changes are necessary when switching between 187 and 395 GHz operation. The most significant of these are the replacements of the back-to-back horns and (if needed) the ferrite rotator.

A schematic of the MAS NMR probe showing the microwave path into the rotor containing the sample is shown in Fig. 3b. The

microwaves are transmitted down the NMR magnet bore through the corrugated waveguide ((g) in Fig. 1) into the top of the probe. This geometry has advantages over the approach used for other systems where a waveguide is attached to the bottom of the probe under the magnet [18,20,24] in that the probe can be easily installed and removed (a tapered guide allows quick and precise connection) and that the waveguide does not use valuable room inside the probe body. The microwaves exit from the corrugated waveguide and pass through a PTFE window in the cryostat before being projected by two mirrors into the top of the MAS rotor, whose outer and inner diameters are 4.0 mm and 2.9 mm respectively. Ideally the optics feeding the microwave beam (in the HE_{11} mode) from the waveguide to the sample would be fully frequency independent and form a constant beam-waist size at the top of the rotor. This insensitivity to source frequency can be achieved by placing refocusing elements (off-axis ellipsoidal mirrors) at sums of focal lengths with their ratio giving the reduction in beam-waist size required to go from the 12.7 mm aperture to the much smaller size needed at the rotor entrance. Space limitations within the probe meant that complete frequency independence could not be achieved, nevertheless the beam-waist formed by the two mirrors is smaller than the inner radius of the rotor at the top rotor cap for both 187 GHz, (1.2 mm) and 395 GHz (0.8 mm).

The beam passes through the cap and a Teflon spacer (~ 8 mm in total), both of which are hollow for most of their lengths, before reaching the sample. The beam characteristics were designed such that in free space the waist for 395 GHz would approximately match the diameter of the silicon-nitride rotor at the top of the sample and is approximately twice this at the bottom (the sample length is 8.7 mm). The 187 GHz beam waist is $\sim 1/3$ larger throughout the rotor.

The MAS probe is triple tuned for NMR, i.e. can operate at three radio frequencies simultaneously; its low temperature operation has been described previously [25]. It has a ^1H channel (550–620 MHz) that covers a wider range than usual for operation at 14.1 T because the magnetic field strength must be adjusted to match the electron spin resonance frequency, an X channel that covers 145–287 MHz and a Y channel that covers 30–84 MHz. This means that the probe can be used with the 395 GHz gyrotron mode as an ^1H -X-Y probe at 14.1 T for 600 MHz ^1H NMR, e.g. ^1H - ^{13}C - ^{15}N with 110 kHz ^1H decoupling, and with the 187 GHz gyrotron mode as an ^1H -X probe at 6.7 T for 287 MHz, e.g. ^1H - ^{13}C with 80 kHz ^1H decoupling. It is necessary for DNP operation for the probe to be able to operate at significantly lower temperatures than a standard MAS NMR probe, preferably 100 K or lower whilst spinning the rotor at several kHz. This has required considerable development in collaboration with Doty Scientific Inc. that has included direct measurement of the sample temperature [25].

The NMR spectrometer is a standard (2008) Varian 3-channel spectrometer except that the magnet and RF amplifiers are

designed for a range of magnetic fields up to 14.6 T, which corresponds to a 620 MHz ^1H NMR frequency. The magnet has an additional coil for sweeping the field strength by ± 0.05 T without opening the persistent mode switch on the main coil, thus conserving liquid helium. This sweep coil also has a persistent mode switch and allows finer adjustments to be made to the field strength than are usually possible with main coils alone. The system therefore allows the field to be set to correspond to a range of EPR and gyrotron frequencies.

3. Experimental details

3.1. Microwave irradiation

The gyrotron microwave mode pattern and the profile of the beam during its transmission by the quasi-optical system were measured using a thermal imaging camera and liquid-crystal-covered Mylar sheets. Powers were measured using a pyro-detector after the back-to-back horns and confirmed by measuring the increase in the temperature of a water load.

Although the maximum DNP-enhancement for a given microwave power would be obtained using CW irradiation of the sample, the gyrotron described in this work gave more power and was more stable in pulsed mode. The output of the gyrotron was controlled by the NMR spectrometer console during DNP MAS NMR experiments with the output power and duty cycle being adjusted to give the largest reproducible enhancement. This paper concentrates on DNP MAS NMR at 6.7 T where the microwave power currently available gives significant DNP enhancements, whilst work at 14.1 T will be presented in a later paper when more microwave power with higher stability is available.

The enhancement, ε_D , for a gyrotron in pulsed mode with duty cycle $D_{\text{MW}} = \tau_D/T_D$, where τ_D is the length of the microwave pulse and T_D is the period of the pulses, can be described by the time derivatives $\varepsilon'_D = (\varepsilon_{\text{CW}} - \varepsilon_D)/T_{1l}$ during the microwave irradiation and $\varepsilon'_D = -\varepsilon_D/T_{1l}$ in its absence. ε_{CW} is the enhancement for CW microwaves for enhancement times $t \gg T_{1l}$ and the characteristic time of build-up and decay of nuclear polarisation is assumed to be dominated by T_{1l} , the nuclear spin lattice relaxation time. An equilibrium is reached for $t \gg T_{1l}$ when the increase during a pulse and decrease during the delay are equal. When T_D is small (but not negligible) compared to T_{1l} then an approximate value can be calculated for ε_D at the end of the microwave pulse using Eq. (2) (see [Supplementary information](#)).

$$\varepsilon_D \approx \varepsilon_{\text{CW}} D_{\text{MW}} \left(1 + \frac{T_D - \tau_D}{2T_{1l}} \right) \quad (2)$$

For larger values of T_D/T_{1l} the enhancement immediately after a pulse increases as the CW regime is approached, and when $T_D/T_{1l} \ll 1$ the fast-pulsing regime is reached and the value of ε_D is decreased to that given by the following equation.

$$\varepsilon_D \approx \varepsilon_{\text{CW}} D_{\text{MW}} \quad (3)$$

In this work experiments typically used several pulses of ~ 1 W at 2 Hz ($T_D = 0.5$ s) and $D_{\text{MW}} = 0.70$ with 15 s between these pulse trains. This configuration was found to produce strong enhancements whilst maintaining gyrotron stability.

3.2. Samples

The TOTAPOL biradical used for the urea and glycine samples described below was synthesised from 4-hydroxy TEMPO using the method of Song et al. [26] and was purified by column chromatography (dichloromethane/methanol (95:5 v/v)) to obtain the TOTAPOL with > 90% yield. The molecular mass measured by mass

spectrometry (ESI) was 400.3179 (m/z [M + H] + $\text{C}_{21}\text{H}_{42}\text{N}_3\text{O}_4^+$ requires 400.3170).

DNP NMR of frozen urea, glucose and glycine samples were performed using 2M ^{13}C urea (99%, Cambridge Isotope Laboratories Inc.), 2M ^{13}C glucose (99% $\text{U-}^{13}\text{C}_6$, Cambridge Isotope Laboratories Inc.) and 1M ^{15}N glycine (98%, ISOTEC) in glycerol- d_8 , D_2O and H_2O (60:30:10 by volume) with 40 mM TOTAPOL. The sample volumes were typically 50 μl .

The bacteriorhodopsin in purple membrane (bR in PM) [27] sample was uniformly ^{13}C labelled and suspended in a minimal amount of buffer composed of 40% by volume of 20 mM sodium citrate pH 6, and 60% deuterated glycerol with 15 mM TOTAPOL. The total sample volume was approximately 40 μl .

3.3. DNP MAS NMR spectroscopy

The DNP MAS NMR probe was tuned for use at 6.7 T with the X channel used for ^1H (283.8 MHz) and the Y channel for ^{13}C (71.4 MHz) or ^{15}N (28.8 MHz). Ramped Cross Polarisation (CP) experiments with up to 70 kHz ^1H decoupling were used. The ^{15}N spectra were referenced relative to CH_3NO_2 [28] and ^{13}C spectra were referenced relative to TMS. Samples were spun in rotors at rates between 4.6 and 5 kHz at 90 K with a typical short-term stability of 10 Hz. The urea, glucose and glycine samples described above were liquid at room temperature and were frozen whilst spinning at approximately 500 Hz, cooling from 290 K to 120 K in <20 s to produce the required glassy structures. The MAS bearing and drive gas temperatures were measured with thermocouples prior to their entry into the stator and these values were converted to sample temperatures using calibration data obtained with $\text{Sm}_2\text{Sn}_2\text{O}_7$ [25]. Both MAS gas flows are used for cooling and were kept at the same temperature to give excellent temperature homogeneity throughout the sample, with the variation being ≤ 1 K [25]. The ability to operate at low temperature is important because both CE and TM DNP enhancements have strong temperature dependences, for instance Rosay et al. [20] found the enhancement more than doubled when the temperature was decreased from 120 to 100 K for a urea sample similar to that used here.

The magnetic field strength of the NMR magnet was adjusted to the maximum positive ^1H DNP enhancement for the TOTAPOL radical. An example of a field sweep using the frozen urea solution is shown in the [Supplementary information](#) (Fig. S4). The internal sweep coil facilitated easy field changes so this process, which included changing the field and re-tuning the NMR probe, typically took only 1–1½ h.

The usual rotor configuration (Fig. 4) consists of, from the top down, a top cap, spacer, sample space, spacer and bottom cap. Silver foil of thickness 0.5 μm was attached to the top surface of the bottom spacer to increase the enhancement and to improve the uniformity of enhancement throughout the sample. This foil thickness is thinner than the penetration depth for NMR frequencies but thicker than that for microwave frequencies. Experiments performed to determine the effects of the silver foil were conducted in two different ways. The initial experiments without the silver foil were conducted by removing the end spacers and putting a spacer in the centre to create two sample spaces (Fig. 4a). One sample space was filled with a urea sample (^{13}C shift ~ 165 ppm) and the other with a glucose sample (^{13}C shift 60–100 ppm). Thus the enhancements at the different positions could be determined. Experiments were performed with the samples in one configuration and then reversed so as to remove the effect of gyrotron instabilities and the differing enhancement with sample. The experiment was repeated with silver foil in place. However as it was not possible to attach the silver foil directly to the bottom cap experiments were conducted with top and bottom spacers in place and a smaller split sample area (Fig. 4b).

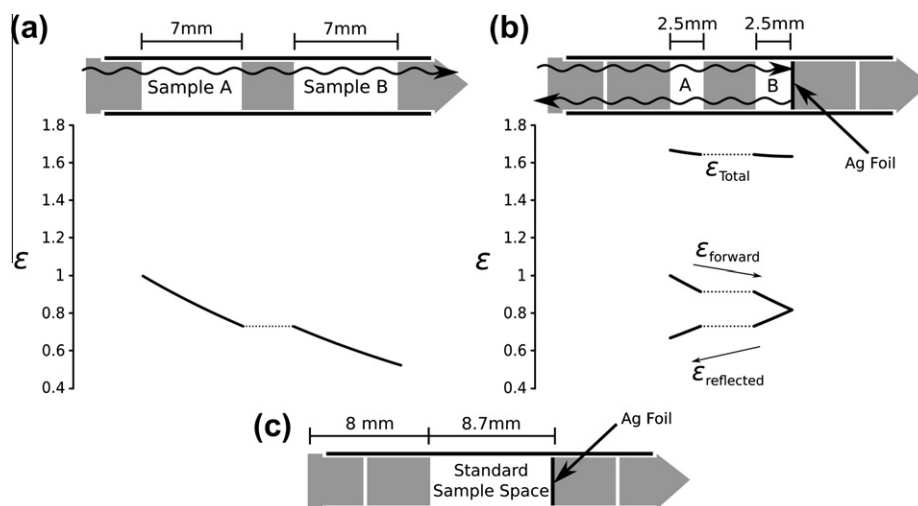


Fig. 4. Model of microwave absorption along the rotor showing the enhancement using samples at different positions in the rotor. The rotor configurations are shown above each plot. The enhancement has been normalised to 1 at the top surface of the sample. It is assumed that the enhancement is directly proportional to power: (a) with no reflective coating at the bottom of the rotor, (b) with silver foil placed on the bottom spacer. The enhancement due to the forward and reflected microwaves is shown together with the total enhancement (which is the sum of $\epsilon_{\text{forward}}$ and $\epsilon_{\text{reflected}}$), (c) shows the configuration for normal operation.

4. Results

Qualitative measurements of the microwave beam at the sapphire window of the gyrotron using liquid-crystal backed Mylar sheets and a thermal imaging camera showed the expected TE_{13} and TE_{16} mode patterns. The Vlasov antenna produced a predominantly Gaussian beam that had focal points of the beam at the correct locations and progressed through the optics to the entrance of the corrugated waveguide. Quantitative measurements showed that the microwave beam power after the back-to-back horns was ~ 1 W, which was similar to that at the first focal point after the antenna.

An example of the build-up of the ^1H - ^{13}C CP DNP MAS NMR signal with successive microwave pulses is shown for the frozen ^{13}C urea solution in Fig. 5, which has a characteristic build-up time (T_{1l} in Eq. (2)) of 3.6 s. Fig. 4 shows the decrease in the enhancements with distance along the MAS rotor that was modelled using data from the double-sample (glucose and urea) experiments. These data are described in more detail in the Discussion. Examples of DNP-enhanced solid-state MAS NMR spectra acquired at 6.7 T using the hardware presented above with the silver foil in place are shown in Figs. 6–8.

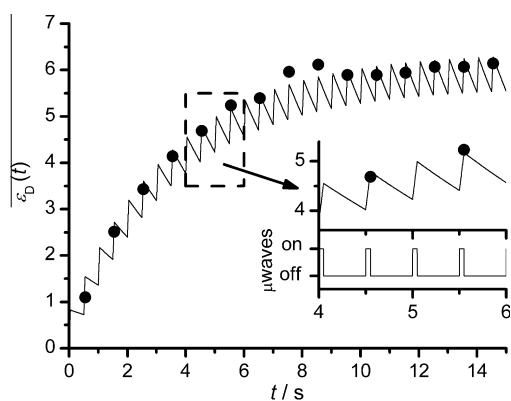


Fig. 5. The build-up of ^1H - ^{13}C CP DNP MAS NMR signal with successive microwave pulses for 2 M ^{13}C urea with 40 mM TOTAPOL at 90 K and 6.7 T. Measurements were taken for even numbers of pulses. $T_D = 0.5$ s, $D_{\text{MW}} = 0.10$, $\epsilon_{\text{CW}} = 60$, characteristic build-up time (T_{1l}) is 3.6 s. Inset: expansion of the region indicated in the main figure (top) with the relative positions of the pulses (bottom).

Fig. 6 shows ^1H - ^{13}C CP MAS spectra for the frozen ^{13}C urea solution. The peak near 165 ppm is that for urea and a DNP enhancement $\epsilon_D = 60$ was achieved using 10 microwave pulses with $D_{\text{MW}} = 0.70$ and $T_D = 0.5$ s. The two peaks between 60 and 80 ppm are those for the natural abundance ^{13}C in the glycerol whose enhancement is unknown because this signal is too weak to be detected in the unenhanced spectrum.

Fig. 7 shows the enhancement obtained using $D_{\text{MW}} = 0.70$, $T_D = 0.5$ s and five pulses for ^1H - ^{15}N CP MAS for the frozen ^{15}N glycine solution to demonstrate the multi-nuclear NMR capability of the DNP-MAS probe. The observed enhancement is $\epsilon_D = 22$. A DNP-enhanced ^1H - ^{13}C CP MAS spectrum for bR in PM is shown in Fig. 8 where an enhancement $\epsilon_D = 16$ was achieved using a similar microwave pulse train.

5. Discussion

The DNP-enhanced solid state MAS NMR spectrometer described here has several important design differences to other recently reported spectrometers [18–20,29] and the relative effectiveness of the different designs will now be discussed.

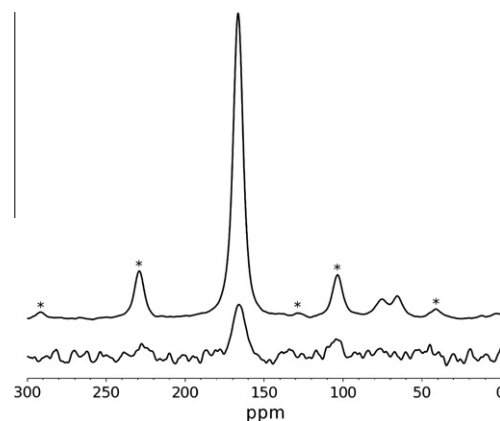


Fig. 6. Comparison of ^1H - ^{13}C CP NMR signal of ^{13}C urea at 90 K and 6.7 T with and without microwave irradiation. Top: 4 acquisitions with microwaves. Bottom: 4 acquisitions without microwaves ($\times 10$). Microwaves applied as 10 pulses with $D_{\text{MW}} = 0.70$ and $T_D = 0.5$ s. The enhancement achieved is ~ 60 . Peak at ~ 165 ppm is urea, the two peaks at around 70 ppm are natural abundance glycerol. Peaks labelled * are spinning sidebands.

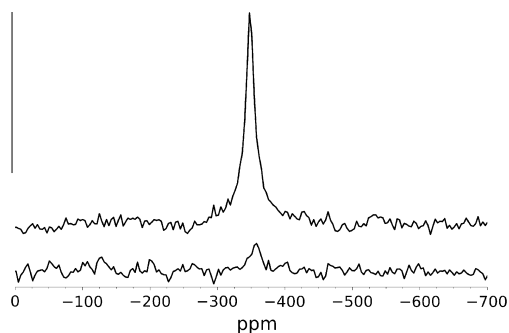


Fig. 7. Comparison of ^1H - ^{15}N CP NMR signal of ^{15}N glycine with 40 mM TOTAPOL at 90 K and 6.7 T with (top, 16 acquisitions) and without (bottom, 128 acquisitions) microwave irradiation. Microwaves applied as 5 pulses with $D_{\text{MW}} = 0.70$ and $T_D = 0.5$ s. Enhancement achieved is ~ 22 .

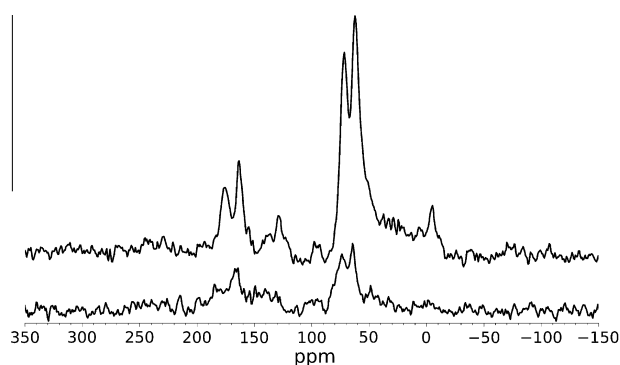


Fig. 8. Comparison of ^1H - ^{13}C CP NMR signal of ^{13}C bacteriorhodopsin in PM with 15 mM TOTAPOL at 90 K and 6.7 T with (top, 100 acquisitions) and without (bottom, 1000 acquisitions) microwaves. Microwaves applied as 5 pulses with $D_{\text{MW}} = 0.70$ and $T_D = 0.5$ s. Enhancement achieved is ~ 16 .

The enhancements presented in this paper are not as large as some of those published for similar experiments because of the need to use the gyrotron in quasi-CW or pulsed mode with limited excitation times (rather than true CW operation) which reduces the maximum enhancement achievable. It is, however, informative to extrapolate the enhancements achieved using Eq. (2) and the modelling described in the [Supplementary information](#) to determine the effectiveness of the microwave transmission system and in particular the method for irradiating the sample in comparison to those of other systems. For the urea sample, with 1 W microwave power, an increase in the number of stable pulses to lengthen the irradiation period to >20 s would have increased the enhancement from 60 to 80, whilst if CW irradiation was available then an enhancement of 115 ± 15 would have been achieved with the same power. This is comparable to the values published for similar samples despite the lower microwave power used here: 165 with 10 W [26] and 190 with 1.5 W [30] at 5 T, and 80 with 6 W at 9.4 T [20]. The variations in the enhancement caused by the differences in the sample composition in these studies are not expected to be as large as those caused by the differences in microwave power, sample temperature and magnetic field strength. Whilst enhancements are expected to reduce with increasing magnetic field strength at these fields with $\epsilon \propto B_0^{-1}$ [6], this reduction has not been quantitatively confirmed experimentally because of the single microwave frequency previously available for each spectrometer. This is a matter that could be addressed using the multiple-field DNP NMR spectrometer design presented here when the power and stability of the higher gyrotron harmonic is improved.

An analysis using a similar polarisation build-up time for ^{15}N -glycine (^1H - ^{15}N CP) gives an increase in the enhancement from 22 to ~ 60 with CW irradiation. For bR in PM (^1H - ^{13}C CP) the increase would be from 16 to ~ 45 (assuming the polarisation build-up time is the same as for the urea sample). The enhancements measured and extrapolated for these samples cannot be compared directly with data published previously as none have been published for ^1H - ^{15}N CP for glycine whilst for bR in PM ^{13}C has been indirectly detected in 2D correlation experiments after ^1H - ^{15}N and then ^{15}N - ^{13}C CP [19,31–33]. Triple-channel NMR experiments are not possible with the MAS probe described above at 6.7 T and we have found that different excitation routes can yield different enhancements, e.g. ^1H MAS NMR often shows significantly smaller DNP enhancements than ^1H - ^{13}C CP MAS NMR.

The most important difference between the DNP-MAS-NMR spectrometer described in this work and those presented previously is the direction and nature of the microwave irradiation at the sample. The different designs used for irradiation have been broadly classified into two types: those where the direction of incidence is approximately along the MAS rotation axis (which is concentric with the solenoidal NMR coil axis) and those where it is perpendicular to that axis (and through the side of the NMR coil) [6]. However, the method of launching the beam into the sample must also be considered.

Close proximity of the solenoidal coil to the rotor is needed for good RF performance and makes beam incidence along the coil and therefore rotation axis an obvious choice. This configuration was used by Afeworki et al. [34] at 1.4 T and early work by Griffin and co-workers [35] utilised such a design at 5 T. In the latter case, a fundamental waveguide bent to the magic angle emitted microwaves at the top of the rotor and a copper mirror at the far end of the stator could be adjusted to maximise the DNP enhancement. However, in their later designs [24] they used a similar configuration to that used by Wind et al. [2] at 1.4 T, with microwave irradiation perpendicular to the rotation axis. This gave superior performance which they attributed to a reduction in the attenuation in samples with typical geometries for MAS (cylinders whose diameters are smaller than their lengths) [6,29].

Previous designs for rotation-axis incidence have relied on attempts to form cavities around rotors using NMR coils and end mirrors. The distribution of microwaves inside such a volume will become increasingly complicated as the wavelength is decreased to a length-scale similar to that for the coil spacing (~ 1 mm), leading to significant scattering losses. Analyses of these designs lead to the decision that their poor behaviour could be attributed to the improper launching of the microwaves and that a design including a quasi-optical beam would eliminate these problems at higher frequencies. The system presented here was therefore designed from the outset to irradiate samples with a focussed Gaussian beam directed along the rotor axis to efficiently couple power into the sample over a broad frequency range. The problems associated with possible losses in the sample are discussed later.

The quasi-optical approach ensures that a single-mode is delivered to the sample and in principle allows the coupling to the sample to be modelled and optimised. This is more challenging in other designs using over-moded waveguides with bends and tapers where there is often significant higher order mode excitation and mode mixing. Matsuki et al. [18] recently utilised over-moded smooth circular waveguide for a rotation-axis approach at 14.1 T. The microwave power at the sample was 5 W (CW) but the ^1H enhancement was limited to ~ 10 for a static frozen glucose solution. This relatively small enhancement might be attributable to the temperature of the sample without microwave irradiation, to heating of the sample by the microwave irradiation and to the high magnetic field strength, but the relatively simple design would have produced complicated scattering of the microwaves near

the sample that makes the results difficult to compare to those from similar work.

Recent work by Nanni et al. [29] investigated the microwave field in the vicinity of the sample for microwaves incident through the NMR coil. Whilst the scattering effect of the NMR coil for their design causes variation of the microwave power throughout the sample, the direction of incidence that is used in our system could suffer from greater absorption of the beam as it propagates through the sample.

As described earlier we have made simple measurements of DNP-enhancement factors using glucose and urea samples (which have different ^{13}C NMR shifts) located in different parts of the rotor (see Fig. 4). The variation of enhancement along the rotation axis was measured as described above with the power being limited to ensure that saturation was unimportant. The normalised enhancements for the bottom of the rotor compared to 1.00 at the top, were 0.75 (urea) and 0.66 (glucose) without the silver foil, and 0.99 (urea) and 1.00 (glucose) with it. The values were averaged to give 0.71 ± 0.15 without and 0.99 ± 0.12 with the silver foil, (errors were calculated using 10% error in the raw enhancement data). (DNP-enhanced spectra that demonstrate the near independence of the enhancement on the position of the sample when using the silver foil are shown in Fig. S5 of the Supplementary information.) These data, which represent the mean enhancement for each part of the rotor, were used to calculate the exponential decay with distance. Fig. 4 illustrates this decay, where the values (for incoming microwaves) have been re-scaled to 1.00 at the top of the upper samples. The effect of attenuation and scattering in the sample has been modelled using $\varepsilon(x) = \varepsilon(0)\exp(-\mu x)$ where x is the position along the rotor axis (in mm) and μ is the attenuation coefficient. This model assumes lossless spacers and total reflection from the silver foil as shown in Fig. 4b. Although the model is unlikely to be completely accurate, it agrees with the data obtained using a single attenuation coefficient, with $\mu = 0.045 \text{ mm}^{-1}$. Assuming that ε is approximately proportional to power at the levels used, i.e. $\leq 1 \text{ W}$, the beam power will have decreased by $\sim 50\%$ by the far end of the test sample (Fig. 4a). The DNP enhancement was therefore found to decrease with a characteristic length of $\sim 20 \text{ mm}$ in our samples which would give a 45% loss of power along the 12.5 mm sample used by Nanni et al. in approximate agreement with the results they published. The rotors we use have the same outside-diameter and a similar sample volume (57 μl in the standard configuration, Fig. 4c) to that used by Nanni et al. but a shorter sample length (8.7 mm). Therefore without the silver foil 70% of the microwave power was transmitted though our samples and the average enhancement was 83% of that for an unattenuated parallel beam (without a reflector). These data suggest that, as expected, the microwaves remain in a beam whose diameter is similar to that of the sample and even smaller than the free-space calculation used for the design. The NMR coil and the surfaces of the rotor, rotor caps and spacers are expected to reflect microwaves back into the sample but, as discussed earlier, it is important for the beam to be launched into the rotor correctly for this direction of incidence to be efficient.

With the silver foil reflector fitted the average enhancements for the top and bottom halves of the sample region were found to be approximately equal, with total enhancement typically being increased by $\sim 70\%$. The average enhancement for the above samples with this reflector is therefore approximately 140% of that for a lossless sample with no reflector due to the increased effective microwave B_1 . The increase in enhancement implies we are still firmly in the regime where we are not saturating the electron spin system and therefore more power should continue to improve the enhancements.

Both the magnetic field strength and sample composition used differ between this study and that by Nanni et al. but their predicted enhancement for 1 W CW microwave irradiation is approx-

imately 50 whilst the experiment described above achieved 60 despite the use of pulsed microwaves with limited irradiation time. We therefore conclude that the configuration with a focussed beam incident along the rotation axis and an end reflector is at least as efficient for generating DNP as that involving irradiation through the NMR coil. The poor performance of other designs using this direction of incidence was therefore caused by inefficient launching of the microwaves into the sample. However, higher duty factors and longer irradiation periods must be used for a quantitative comparison and work is underway to achieve these with 187 GHz and higher-frequency microwaves.

The irradiation of the sample along the MAS rotation axis has a number of advantages over that through the NMR coil if the efficiencies are similar, including (i) that the coil has a relatively simple role and the sample area can therefore be more easily modified to increase the microwave intensity, (ii) that the use of smaller rotors for faster MAS can be implemented with coils designed for optimal NMR sensitivity rather than requiring that the coil-wire spacing be dependent on the microwave wavelength, (iii) that absorption of the microwaves by the wall material of the rotor is less important thus it is not necessary to use relatively fragile sapphire rotors, and (iv) that comparisons of enhancements using two gyrotron harmonics can be more easily made when the wavelength-dependent scattering by the coil is less important. The current DNP MAS NMR probe design does not provide access for a rotor-insert/eject system but the general design does not prohibit this, and in our system the time required to change samples is only $\sim 1 \text{ h}$ (including warming and re-cooling the probe).

The quasi-optical microwave transmission system used here differs to that used for other high-field DNP MAS NMR spectrometers in its efficiency, controllability and versatility throughout the transmission of microwaves from the gyrotron. The Vlasov antenna can only launch certain types of mode into the optics and only one well defined mode pattern will be correctly focussed into the back-to-back horns for a particular antenna configuration, i.e. the distance from the launcher to the elliptical mirror (M1 in Fig. 3a) and the orientation of the adjustable parabolic mirror (M2). Unwanted modes will therefore not be transmitted, thus reducing unnecessary sample heating. Only a small frequency range is supported without movement of the parabolic mirror, thus the microwaves transmitted can be controlled, but gyrotron instabilities could be exacerbated. The optics after this adjustable mirror were designed so that very little adjustment need or can be made without removal or replacement of components. The design has many other advantages including (i) that the power and polarisation of the microwaves can be monitored and controlled, (ii) that after conversion to a Gaussian beam the losses in power are very small even over the relatively large distances between superconducting magnets, and (iii) that with replacement of only the back-to-back horns and the Faraday rotator it can be used at very different frequencies allowing both the fundamental and second-harmonic modes to be used. The dependence of the DNP enhancement on the power can be easily determined without changing the operating parameters for the gyrotron, modification of which can cause very non-linear responses, and the optics can also be easily modified for other uses such as a basic EPR system for calibrating the magnetic field to achieve optimal DNP enhancements. However, it is relatively complicated to set up the Vlasov antenna, and its efficiency, in combination with the waveguide leading to it, is very sensitive and intolerant to misalignments. For instance, if the offset between the gyrotron and the launcher mount is $>1^\circ$ then parts of the microwave beam could miss mirror 6 (Fig. 2). Furthermore for the microwaves to be effectively launched the output of the gyrotron needs to be the correct high purity single mode. Note, for general use the beam must be enclosed for safety reasons as even if it propagates correctly the second harmonic frequency is classified as

far infra-red (IR-C) and the focussed fundamental mode beam could have a power density of up to 300 W/cm².

The use of the second-harmonic of a gyrotron reduces the power available whilst requiring operating conditions that can cause decreased stability and reliability. The specifications for the second harmonic of the gyrotron used here include maximum powers similar to those commonly used for DNP (≤ 10 W [20,26,30]) but operation must be simultaneously achieved with the stability needed for DNP-NMR. It is perhaps because of this necessity for both high power and stability that gyrotrons operating in second-harmonic modes have seldom been used for DNP NMR, with only Matsuki et al. [18] having successfully used such a gyrotron, which was similar to that used here. The ability of the frequency-independent hardware described above to use both harmonics with only relatively simple modifications is therefore advantageous to understanding the level of enhancement achievable at different magnetic field strengths. Comparisons could be made between results for the two frequencies to reduce uncertainties caused by factors such as the relatively limited powers available at the higher frequency. The new ideas introduced here (e.g. using quasi-optical transmission from a gyrotron source for irradiation along the MAS rotor axis) increase the range of possibilities as new high field DNP spectrometers are developed. The flexibility of the current design to accommodate a switch between frequencies means that multi-frequency high field DNP spectrometers for solid state NMR are feasible.

6. Conclusions

The DNP system presented in this paper uses a unique combination of quasi-optics with a focussed microwave beam and a high-power microwave source. The quasi-optical microwave transmission has many advantages over waveguide including the broad frequency range over which the system can operate and low power losses even over large distances. It allows more detailed measurements of the microwave transmission to be made but the initial set-up is more difficult and the optics would need to be enclosed in a system for general use. The enhancements obtained at 6.7 T using this system are similar to those obtained using similar DNP MAS NMR spectrometers, but calculations suggest that the enhancement would be significantly larger if a higher stable power output was available. The field dependence of these enhancements could be measured using the fundamental and second-harmonic frequencies of the gyrotron with only minor modifications when more power and stability is available for the latter. The microwave beam is incident along the MAS rotation axis, focussed near the top of the sample, and has a beam profile not much larger than the sample diameter. This geometry had been discounted by most other groups but, as shown here, such irradiation is efficient, provides relatively uniform enhancement throughout the sample and its simplicity allows RF coils optimised for NMR to be used.

A modest enhancement of 16 with only ~ 1 W microwave power at 6.7 T was measured for bR in PM, which equates to a reduction of experimental time by a factor of 256. The Boltzmann factor and reduced thermal noise at 90 K provide a further gain of ~ 4 compared to room temperature operation, giving a potential total reduction of experimental time of ~ 4000 . With the continuing development of DNP techniques and related hardware DNP-NMR is becoming more routine and applicable to a larger range of materials, opening many new fields for research to solid state NMR approaches.

Acknowledgments

This work was supported by EPSRC (UK) Basic Technology Project Grants EP/D045967 and EP/D047730. We thank Doty Scientific Inc. for their cooperation in the development of the MAS NMR

probe, Adrian Lovejoy and David Greenshields of the Electronics Workshop in the Department of Physics at the University of Warwick, and the NMR Magnet Group in The Magnet Technology Centre at Agilent Technologies UK Ltd. Thomas K.Y. Tam (Warwick) is thanked for running and analysing X-band EPR spectra.

Appendix A. Supplementary material

Supplementary data associated with this article can be found, in the online version, at doi:10.1016/j.jmr.2011.12.006.

References

- [1] A.W. Overhauser, Polarization of nuclei in metals, *Phys. Rev.* 92 (1953) 411–415.
- [2] R.A. Wind, M.J. Duijvestijn, C. Vanderlugt, A. Manenschijn, J. Vriend, Applications of dynamic nuclear polarization in ¹³C NMR in solids, *Prog. Nucl. Magn. Reson. Spectrosc.* 17 (1985) 33–67.
- [3] E. Erb, J.L. Motchane, J. Uebersfeld, Résonance Nucléaire – Effet de polarisation nucléaire dans les liquides et les gaz adsorbés sur les charbons, *C.R. Hebd. Seances Acad. Sci.* 246 (1958) 2121–2126.
- [4] A. Abragam, W.G. Proctor, Résonance Nucléaire – Une nouvelle méthode de polarisation dynamique des noyaux atomiques dans les solides, *C.R. Hebd. Seances Acad. Sci.* 246 (1958) 2253–2256.
- [5] D. Sezer, M.J. Prandolini, T.F. Prisner, Dynamic nuclear polarization coupling factors calculated from molecular dynamics simulations of a nitroxide radical in water, *Phys. Chem. Chem. Phys.* 11 (2009) 6626–6637.
- [6] T. Maly, G.T. Debelouchina, V.S. Bajaj, K.-N. Hu, C.-G. Joo, M.L. Mak-Jurkaskas, J.R. Sirigiri, P.C.A. van der Wel, J. Herzfeld, R.J. Temkin, R.G. Griffin, Dynamic nuclear polarization at high magnetic fields, *J. Chem. Phys.* 128 (2008) 052211.
- [7] A.V. Kessenikh, V.I. Lushchikov, A.A. Manenkov, Y.V. Taran, Proton polarization in irradiated polyethylenes, *Sov. Phys. Solid State* 5 (1963) 321–329.
- [8] C.F. Hwang, D.A. Hill, New effect in dynamic polarization, *Phys. Rev. Lett.* 18 (1967) 110–112.
- [9] C.F. Hwang, D.A. Hill, Phenomenological model for the new effect in dynamic polarization, *Phys. Rev. Lett.* 19 (1967) 1011–1014.
- [10] B.N. Provotorov, Magnetic resonance saturation in crystals, *Sov. Phys. JETP* 14 (1962) 1126–1131.
- [11] C. Ysacco, E. Rizzato, M.A. Virolleaud, H. Karoui, A. Rockenbauer, F. Le Moigne, D. Siri, O. Ouari, R.G. Griffin, P. Tordo, Properties of dinitroxides for use in dynamic nuclear polarization (DNP), *Phys. Chem. Chem. Phys.* 12 (2010) 5841–5845.
- [12] K.R. Thurber, W.-M. Yau, R. Tycko, Low-temperature dynamic nuclear polarization at 9.4 Tesla with a 30 milliwatt microwave source, *J. Magn. Reson.* 204 (2010) 303–313.
- [13] J.H. Ardenkjaer-Larsen, B. Fridlund, A. Gram, G. Hansson, L. Hansson, M.H. Lerche, R. Servin, M. Thaning, K. Golman, Increase in signal-to-noise ratio of $>10,000$ times in liquid-state NMR, *Proc. Natl. Acad. Sci. U.S.A.* 100 (2003) 10158–10163.
- [14] J. Leggett, R. Hunter, J. Granwehr, R. Panek, A.J. Perez-Linde, A.J. Horsewill, J. McMaster, G. Smith, W. Köckenberger, A dedicated spectrometer for dissolution DNP NMR spectroscopy, *Phys. Chem. Chem. Phys.* 12 (2010) 5883–5892.
- [15] A. Krahn, P. Lottmann, T. Marquardsen, A. Tavernier, M.-T. Türke, M. Reese, A. Leonov, M. Bennati, P. Hofer, F. Engelke, C. Griesinger, Shuttle DNP spectrometer with a two-center magnet, *Phys. Chem. Chem. Phys.* 12 (2010) 5830–5840.
- [16] P.A.S. Cruickshank, D.R. Bolton, D.A. Robertson, R.I. Hunter, R.J. Wylde, G.M. Smith, A kilowatt pulsed 94GHz electron paramagnetic resonance spectrometer with high concentration sensitivity, high instantaneous bandwidth, and low dead time, *Rev. Sci. Instr.* 80 (2009) 103102.
- [17] E.V. Kryukov, M.E. Newton, K.J. Pike, D.R. Bolton, R.M. Kowalczyk, A.P. Howes, M.E. Smith, R. Dupree, DNP enhanced NMR using a high-power 94 GHz microwave source. a study of the TEMPOL radical in toluene, *Phys. Chem. Chem. Phys.* 12 (2010) 5757–5765.
- [18] Y. Matsuki, H. Takahashi, K. Ueda, T. Idehara, I. Ogawa, M. Toda, H. Akutsu, T. Fujiwara, Dynamic nuclear polarization experiments at 14.1 T for solid-state NMR, *Phys. Chem. Chem. Phys.* 12 (2010) 5799–5803.
- [19] V.S. Bajaj, M.K. Hornstein, K.E. Kreischer, J.R. Sirigiri, P.P. Woskov, M.L. Mak-Jurkaskas, J. Herzfeld, R.J. Temkin, R.G. Griffin, 250GHz CW gyrotron oscillator for dynamic nuclear polarization in biological solid state NMR, *J. Magn. Reson.* 189 (2007) 251–279.
- [20] M. Rosay, L. Tometich, S. Pawsey, R. Bader, R. Schauwecker, M. Blank, P.M. Borchard, S.R. Cauffman, K.L. Felch, R.T. Weber, R.J. Temkin, R.G. Griffin, W.E. Maas, Solid-state dynamic nuclear polarization at 263 GHz: spectrometer design and experimental results, *Phys. Chem. Chem. Phys.* 12 (2010) 5850–5860.
- [21] T. Idehara, K. Kosuga, L. Agusu, I. Ogawa, H. Takahashi, M.E. Smith, R. Dupree, Gyrotron DU CW VIII for 300 MHz and 600 MHz DNP-NMR spectroscopy, *J. Infrared Millimeter, Terahertz Waves* 31 (2010) 763–774.
- [22] N. Vlasov, L.I. Zagryadskaya, M.I. Petelin, Transformation of a whispering gallery mode, propagating in a circular waveguide into beam of waves, *Radio*

- Eng. Electron. Phys. 20 (1975) 14–17;
S.N. Vlasov, M.A. Shapiro, K.M. Likin, Geometrical optics of waveguide mode converters, *Opt. Commun.* 88 (1992) 455–463.
- [23] D.H. Martin, E. Puppelt, Polarised interferometric spectrometry for the millimetre and submillimetre spectrum, *Infrared Phys.* 10 (1969) 105–109.
- [24] A.B. Barnes, M.L. Mak-Jurkauskas, Y. Matsuki, V.S. Bajaj, P.C.A. van der Wel, R. DeRocher, J. Bryant, J.R. Sirigiri, R.J. Temkin, J. Lugtenburg, J. Herzfeld, R.G. Griffin, Cryogenic sample exchange NMR probe for magic angle spinning dynamic nuclear polarization, *J. Magn. Reson.* 198 (2009) 261–270.
- [25] T.F. Kemp, G. Balakrishnan, K.J. Pike, M.E. Smith, R. Dupree, Thermometers for low temperature Magic Angle Spinning NMR, *J. Magn. Reson.* 204 (2010) 169–172.
- [26] C. Song, K. Hu, C. Joo, T. Swager, R.G. Griffin, TOTAPOL: a biradical polarizing agent for dynamic nuclear polarization experiments in aqueous media, *J. Am. Chem. Soc.* 128 (2006) 11385–11390.
- [27] D. Oesterhelt, W. Stoerkenius, Isolation of the cell membrane of *Halobacterium halobium* and its fractionation into red and purple membrane, *Methods Enzymol.* 31 (1974) 667–678.
- [28] J. Mason, 2007, Nitrogen NMR, *Encyclopedia of Nuclear Magnetic Resonance*.
- [29] E.A. Nanni, A.B. Barnes, Y. Matsuki, P.P. Woskov, B. Corzilius, R.G. Griffin, R.J. Temkin, Microwave field distribution in a magic angle spinning dynamic nuclear polarization NMR probe, *J. Magn. Reson.* 210 (2011) 16–23.
- [30] K.N. Hu, C. Song, H.H. Yu, T.M. Swager, R.G. Griffin, High-frequency dynamic nuclear polarization using biradicals: a multifrequency EPR lineshape analysis, *J. Chem. Phys.* 128 (2008) 052302.
- [31] M. Rosay, J.C. Lansing, K.C. Haddad, W.W. Bachovchin, J. Herzfeld, R.J. Temkin, R.G. Griffin, High-frequency dynamic nuclear polarization in MAS spectra of membrane and soluble proteins, *J. Am. Chem. Soc.* 125 (2003) 13626–13627.
- [32] M.L. Mak-Jurkauskas, V.S. Bajaj, M.K. Hornstein, M. Belenky, R.G. Griffin, J. Herzfeld, Energy transformations early in the bacteriorhodopsin photocycle revealed by DNP-enhanced solid-state NMR, *Proc. Natl. Acad. Sci. U. S. A.* 105 (2008) 883–888.
- [33] V.S. Bajaj, M.L. Mak-Jurkauskas, M. Belenky, J. Herzfeld, R.G. Griffin, Functional and shunt states of bacteriorhodopsin resolved by 250 GHz dynamic nuclear polarization-enhanced solid-state NMR, *Proc. Natl. Acad. Sci. U. S. A.* 106 (2009) 9244–9249.
- [34] M. Afeworki, R.A. McKay, J. Schaefer, Selective observation of the interface of heterogeneous polycarbonate/polystyrene blends by dynamic nuclear polarization carbon-13 NMR spectroscopy, *Macromolecules* 25 (1992) 4084–4091.
- [35] L.R. Becerra, G.J. Gerfen, B.F. Bellew, J.A. Bryant, D.A. Hall, S.J. Inati, R.T. Weber, S. Un, T.F. Prisner, A.E. McDermott, K.W. Fishbein, K.E. Kreisler, R.J. Temkin, D.J. Singel, R.G. Griffin, A Spectrometer for dynamic nuclear polarization and electron paramagnetic resonance at high frequencies, *J. Magn. Reson. A* 117 (1995) 28–40.